The Astrophysical Journal, 551:L115–L119, 2001 April 10

THE MAGNETIC ROPE STRUCTURE AND ASSOCIATED ENERGETIC PROCESSES IN THE 2000 JULY 14 SOLAR FLARE

Yihua Yan,[1] Yuanyong Deng,[1] Marian Karlický,[2] Qijun Fu,[1] Shujuan Wang,[1] and Yuying Liu[1]
Received 2000 October 31; accepted 2001 February 20; published 2001 March 26

ABSTRACT

In the reconstructed nonlinear force-free magnetic field of NOAA Active Region 9077 before the X5.7/3B (10:24 UT) flare on 2000 July 14, we reveal for the first time the presence of a magnetic rope from the extrapolation of the three-dimensional magnetic field structure. This magnetic rope is located in a space above the magnetic neutral lines of the filament. The calculated field lines of the rope rotate around its axis for more than three turns. Overlying the rope are multilayer magnetic arcades with different orientations. These arcades are in agreement with the *Transition Region and Coronal Explorer* observations. The estimated free magnetic energy in this rope system is about 1.6×10^{32} ergs. Such magnetic field structure provides a favorable model for the interpretation of the energetic flare processes as revealed by Hα, EUV, and radio observations. In particular, the intermittent cospatial brightening of the rope in EUV 1600 Å image leading to the onset of the flare suggests that the rope instability may have triggered the flare event, and the drifting pulsation structure in the decimetric frequency range is considered to manifest the initial phase of the coronal mass ejection.

Subject headings: Sun: flares — Sun: magnetic fields — Sun: radio radiation — Sun: UV radiation

1. INTRODUCTION

Magnetic ropes are believed to play an important role in the eruptions of filaments, coronal mass ejection (CME) processes, and flares (Priest 1981; Shibata 1995; Low 1996; Tsuneta 1996). The concept of magnetic ropes has been introduced theoretically and has been used to interpret prominences and CMEs (Low 1992; Plunkett et al. 2000). But, in this Letter, we present for the first time the magnetic rope structure reconstructed from observed vector magnetograms, using a newly developed non–constant α force-free field extrapolation technique (Yan & Sakurai 1997, 2000). We also discuss the associated flare and CME initiation processes as revealed by Hα, EUV, and radio observations.

2. OBSERVATIONS

The 2000 July 14 flare, classified as X5.7/3B, was observed at 10:03–10:43 UT in the NOAA Active Region 9077 at a position N22°, W07°. In connection with this flare, the halo CME, type II and moving type IV radio bursts, and relativistic protons were reported.[3] We employed the vector magnetograms and Hα images taken at the Huairou Station of the Beijing Astronomical Observatory (BAO; Deng et al. 1997), the EUV images taken by the *Transition Region and Coronal Explorer* (*TRACE*; Handy et al. 1999), and the radio observations performed by the newly developed Solar Radio Broadband Dynamic Spectrometers (1–2, 2.6–3.8, and 5.2–7.6 GHz) at Huairou Station of the BAO (Fu et al. 1995) and by the 0.8–2 and 2–4.5 GHz radiospectrographs at the Ondřejov Observatory (Jiřička et al. 1993). Figure 1 shows magnetogram, Hα, and EUV images of the active region before and during the X5.7/3B flare.

The evolution of the photospheric magnetic fields in AR 9077 on 2000 July 14 did not show significant changes before the flare, and we chose the higher quality vector magnetograms taken at 01:19 UT before local meridian time (Fig. 1*a*). No significant new emerging flux region was observed during this period (H. Wang 2000, private communication). However, the negative polarity fields between the two main opposite poles were stretched around 08 UT, and the neutral lines were elongated in the directions indicated by the arrows. The Hα observations indicate that there was a long filament with a triangular shape (Fig. 1*b*); this filament existed for a long time before its right side (above the location marked by the arrow) began to erupt toward the northwest. The EUV 1600 Å image taken by *TRACE* shows a lane patch brightened intermittently before the flare at the lower portion of the Hα filament, where it began to brighten again at 09:22 UT, and the bright lane (marked by the arrow in Fig. 1*c*) was formed at 09:26 UT before the onset of the flare. The high-cadence Hα observations indicate that the northern ribbon was growing from the west to the east, parallel to the neutral line, and was expanding in a perpendicular direction (see, e.g., the bright bulb marked by the black arrow and the ribbon patches in Fig. 1*d*). The separation of the western bright patch into two ribbons was also observed at 10:30:21 UT.

The 0.8–4.5 GHz radio emission of this flare is shown in Figure 2. The first indication of an enhanced radio emission appeared at 10:00–10:07 UT in the 0.8–1.0 GHz frequency range. Then, at 10:24–10:25 UT in the 0.8–3.0 GHz frequency range, the fast drift burst was observed. Its drift was determined to be -240 MHz s^{-1}. After this burst, at 10:24–10:32 UT in the 2.7–4.5 GHz range, the continuum (with the drifting features at its initial phase) was observed. In the lower frequencies in the 0.8–1.5 GHz range at 10:27–10:35 UT, this burst was accompanied by the drifting pulsation structure (DPS). Its frequency drift is -3.3 MHz s^{-1}, and the instantaneous bandwidth is greater than 1 GHz. These radio bursts were observed with the same features at both distant observatories. Finally, in the further phase of the flare, two radio bursts were observed at 10:42–10:45 and

[1] Beijing Astronomical Observatory/National Astronomical Observatories, Chinese Academy of Sciences, 20 Datun Road, Chaoyang Beijing, 100012, China.
[2] Astronomical Institute, Academy of Sciences of the Czech Republic, Dr. Frice 1, Ondřejov, CZ-251 65, Czech Republic.
[3] See http://www.sel.noaa.gov.

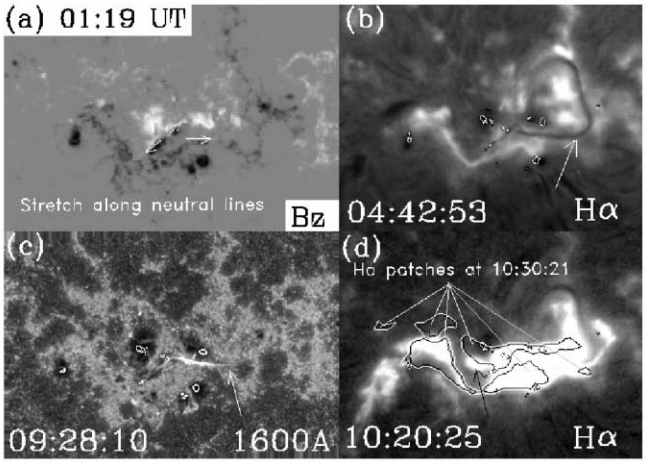

FIG. 1.—(*a*) Huairou mosaic longitudinal magnetogram with white (black) indicating north (south) polarity of more than 3000 G. (*b*) Huairou Hα image showing a long triangle-shaped filament. (*c*) *TRACE* EUV 1600 Å image showing a bright lane in a space above the filament. (*d*) Huairou Hα flare image at 10:20:25 UT, overlaid with flare ribbon patches at 10:30:21 UT. The small contours overlaid on the EUV and Hα images indicate the locations of sunspots. Each panel is about $6' \times 4'$ in size; north is to the top, and west is to the right.

10:46–11:00 UT in the 0.8–1.5 and 0.8–1.7 GHz ranges, respectively.

3. RECONSTRUCTION OF THE MAGNETIC ROPE

The extrapolation code is based on the work of Yan & Sakurai (1997, 2000) so that a non–constant α force-free magnetic field (satisfying $\nabla \times \boldsymbol{B} = \alpha \boldsymbol{B}$) with a finite energy content in open space Ω above the solar surface Γ can be represented by the following boundary integral equation:

$$\boldsymbol{B}(\boldsymbol{r}_i) = \int_\Gamma \left[Y(\boldsymbol{r}_i; \boldsymbol{r}) \frac{\partial \boldsymbol{B}}{\partial n}(\boldsymbol{r}) - \frac{\partial Y}{\partial n}(\boldsymbol{r}_i; \boldsymbol{r}) \boldsymbol{B}(\boldsymbol{r}) \right] d\Gamma, \qquad (1)$$

where $Y(\boldsymbol{r}_i; \boldsymbol{r}) = \cos(\lambda|\boldsymbol{r} - \boldsymbol{r}_i|)/(4\pi|\boldsymbol{r} - \boldsymbol{r}_i|)$ is the proposed fundamental solution, $\boldsymbol{r}_i$ and $\boldsymbol{r}$ are, respectively, a fixed point in Ω and the variable source point on Γ, and $\lambda = \lambda(\boldsymbol{r}_i)$ is a local parameter implicitly defined by the following equation if no currents are at infinity (Yan & Sakurai 1997, 2000):

$$\int_\Omega Y(\boldsymbol{r}_i; \boldsymbol{r})[\lambda^2(\boldsymbol{r}_i)\boldsymbol{B}(\boldsymbol{r}) - \alpha^2(\boldsymbol{r})\boldsymbol{B}(\boldsymbol{r}) - \nabla\alpha(\boldsymbol{r}) \times \boldsymbol{B}(\boldsymbol{r})] d\Omega = 0. \qquad (2)$$

We followed the second approach as described in Yan & Sakurai (2000) in order to avoid solving for λ in equation (2), but we approximately chose λ-values according to the α-distribution on Γ. In this way, $\partial \boldsymbol{B}/\partial n$ over the boundary can be obtained from vector $\boldsymbol{B}$, which is known over Γ as a boundary condition. Then the field at any point in Ω can be calculated by equation (1). Thus, we obtain a numerical approximation of the non–constant α force-free field.

Figure 3 shows the calculated magnetic field lines projected onto the photospheric magnetogram at 01:19 UT. It can be seen that the main features of the magnetic fields are the multilayer magnetic field lines forming arcades with different orientations.

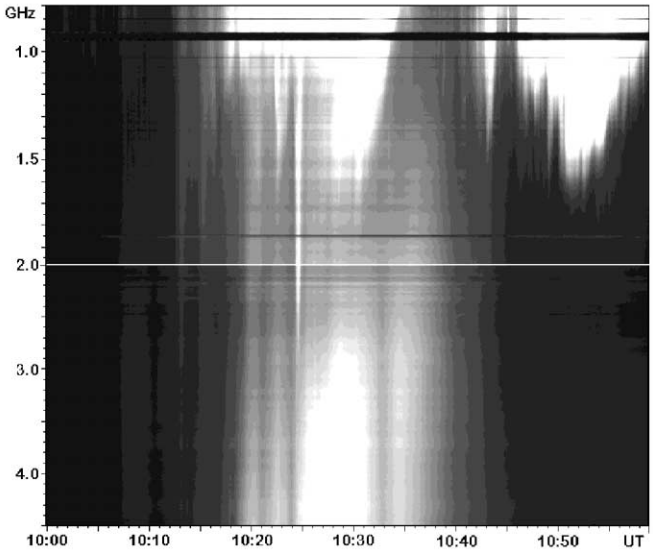

FIG. 2.—The 0.8–4.5 GHz radio emission observed on 2000 July 14 by the Ondřejov radiospectrographs. The dark horizontal bands represent gaps where strong artificial radio sources appeared. The white line at 2 GHz expresses the border between two spectra obtained from two different radiospectrographs (0.8–2.0 and 2.0–4.5 GHz).

Inside this magnetic arcade, there is a magnetic rope suspended in the corona above the stretched neutral lines. The calculated field lines of the rope rotate around its axis for more than three turns.

The three-dimensional structure of the magnetic rope is shown in Figure 4. As marked by the arrows in Figures 1*b* and 1*c*, the right branch of the rope was cospatial with the Hα filament and the EUV bright lane. As indicated in Figure 1*d*, the left branch of the rope was cospatial with the Hα flare bulb at 10:20:25 UT, and furthermore it had the same shape as the bulb. The rope was located at the center of the flare patch as shown in Figure 4*d*. The front and side views are shown in Figures 4*e* and 4*f* as well. From these figures, we see that the reconstructed rope in the chromosphere and low corona has a total projected length of about 100″ and a height ranging from about 2″ to 30″. The rope thickness is about 20″, as shown in Figure 4*f*. The estimated free magnetic energy in this rope system is about 1.6×10^{32} ergs.

4. DISCUSSIONS

Low (1992) proposed a magnetostatic model to obtain the levitated magnetic ropes interpretable as chromospheric filaments. Karlický (1997) considered the force-free currents in ropes in an initial potential field. Aulanier et al. (1999) applied Low's (1992) linear model to the real magnetograms for an explanation of magnetic dips. Amari (2000) simulated the formation of helical fields by MHD. Here we have obtained the magnetic rope, for the first time, from observed vector magnetograms by using Yan & Sakurai's (1997, 2000) technique for non–constant α force-free field problems. The reconstructed magnetic field structures contain exactly the same components as shown in Figure 6 of Low (1992).

For a single loop, the critical stability value of the twist is about 2.5π (Hood 1991). But, in the present case, the twist values of some calculated field lines forming the magnetic rope were found to be above 3.0π, much greater than 2.5π, and they existed about 10 hr before the X5.7/3B flare. This can be ex-

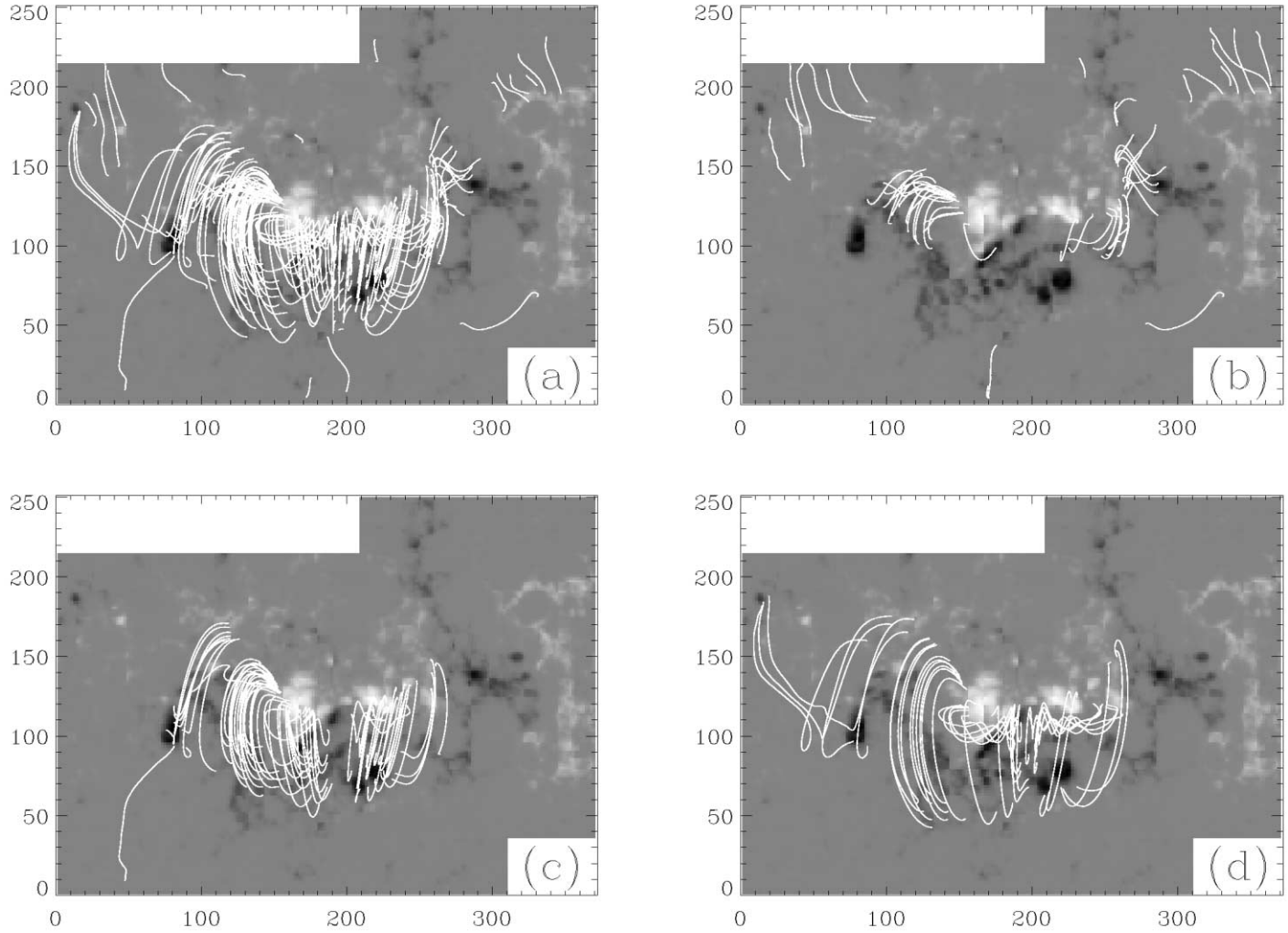

FIG. 3.—Reconstructed magnetic field lines projected onto the photospheric magnetogram of Fig. 1*a*. (*a*) Overall calculated field lines that are closed to the photosphere; (*b*) lower lying lines (2″–25″ high) showing arcades across the neutral lines; (*c*) higher lying lines (25″–50″ high) showing arcades with different orientations; and (*d*) the magnetic rope along the neutral line embraced by overlying arcades. The blank areas are due to the mosaic of the vector magnetograms.

plained by the surrounding arc structure that kept the magnetic rope stable. For the X5.7/3B flare in this active region, no new emerging flux region was found (H. Wang 2000, private communication). Therefore, magnetic shearing, as revealed by the stretch of the neutral lines, may be the cause of the magnetic rope destabilization. The free magnetic energy in this rope system is estimated to be 1.6×10^{32} ergs. Indeed, the 1600 Å bright lane was exactly cospatial with the right branch of the rope, and it brightened intermittently until the onset of the filament eruption and the flare/CME process.

Recently, the DPS observed during the 1992 October 5 plasmoid ejection (Ohyama & Shibata 1998) was explained in Kliem, Karlický, & Benz (2000) by the upward plasmoid motion. As described by Ohyama & Shibata (1998), the plasmoid ejection process is connected with the extended loop (magnetic rope) moving upward. In the present case, the rope was cospatial with the Hα filament, at which location the brightening of the EUV 1600 Å image first occurred, and the whole rope was eventually located in the Hα flare kernel. At 10:20:25 UT, the rope confined an Hα bright bulb with the same shape; this bulb was growing fast from west to east at 10:30:21 UT. Therefore, the DPS observed at 10:27–10:35 UT in the 0.8–1.5 GHz range is most likely interpreted as the radio signature of the plasmoid ejection accompanied by the upward-moving magnetic rope. Since the halo CME was developed from this filament (or rope) eruption, we think that this DPS in the decimetric frequency range manifests the initial phase of the CME.

This work was supported by the Ministry of Science and Technology of the People's Republic of China (G2000078403), the NSFC (19973008, 49990452, 49990451, and 19833050), and the CAS (STORM23). The authors are grateful to the *TRACE* team for providing the observational data, and they thank the anonymous referee for helpful comments. One of the authors (M. K.) thanks the Solar Radioastronomical group of BAO for his invitation and fruitful stay there. This Letter was also partly supported by grant A3003707 of the Grant Agency of the Academy of Sciences, Czech Republic.

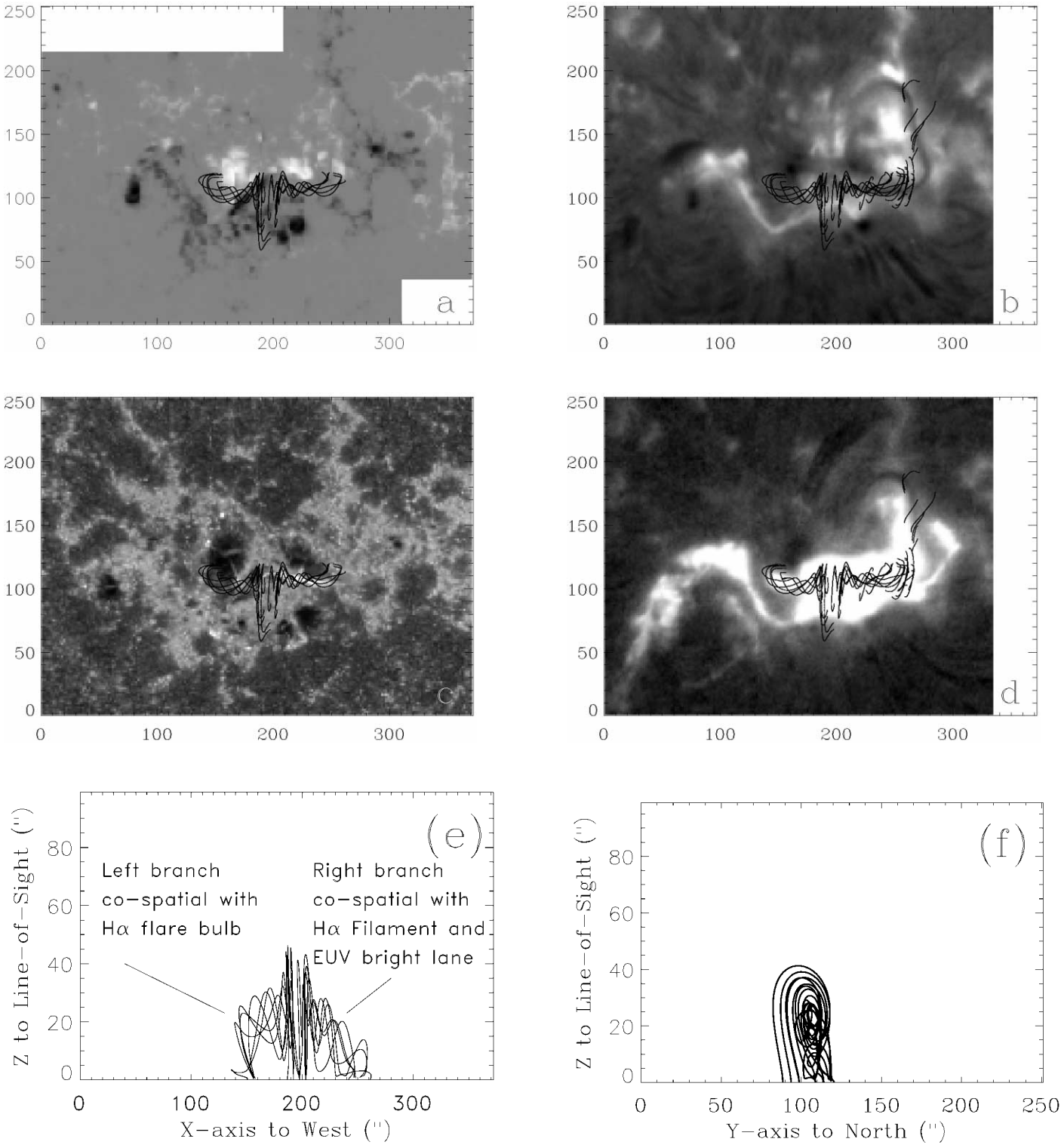

FIG. 4.—Magnetic rope overlaid with the same (*a*) magnetogram, (*c*) EUV image, and (*b*, *d*) Hα images as in Fig. 1. Panels (*e*) and (*f*) are the front and side views of the rope, respectively. Some low-lying field lines (2″–33″ high) forming arcades across the filament are also displayed over the (*b*, *d*) Hα images.

REFERENCES

Amari, T. 2000, ApJ, 529, L49
Aulanier, G., Démoulin, P., Mein, N., van Driel-Gesztelyi, L., Mein, P., & Schmieder, B. 1999, A&A, 342, 867
Deng, Y., Ai, G., Wang, J., Song, G., Zhang, B., & Ye, X. 1997, Sol. Phys., 173, 207
Fu, Q., Qin, Z., Ji, H., & Pei, L. 1995, Sol. Phys., 160, 97
Handy, B., et al. 1999, Sol. Phys., 187, 229
Hood, A. W. 1991, Solar System Magnetohydrodynamics, ed. E. R. Priest & A. W. Hood (London: Cambridge Univ. Press), 307
Jiřička, K., Karlický, M., Kepka, O., & Tlamicha, A. 1993, Sol. Phys., 147, 203
Karlický, M. 1997, A&A, 318, 289
Kliem, B., Karlický, M., & Benz, A. O. 2000, A&A, 360, 715
Low, B. C. 1992, ApJ, 399, 300
———. 1996, Sol. Phys., 167, 217
Ohyama, M., & Shibata, K. 1998, ApJ, 499, 934
Plunkett, S. P., et al. 2000, Sol. Phys., 194, 371
Priest, E. R. 1981, Solar Flare Magnetohydrodynamics (London: Gordon & Breach)
Shibata, K. 1995, Adv. Space Res., 17(4–5), 9
Tsuneta, S. 1996, in ASP Conf. Ser. 111, Magnetic Reconnection in the Solar Atmosphere, ed. R. D. Bentley & J. T. Mariska (San Francisco: ASP), 409
Yan, Y., & Sakurai, T. 1997, Sol. Phys., 174, 65
———. 2000, Sol. Phys., 195, 89